Isothermal, non-oxidative, two-step CH_4 conversion over unsupported and supported Ru and Pt catalysts

Michael C.J. Bradford

CeraMem Corporation, 12 Clematis Avenue, Waltham, MA 02453, USA
E-mail: mbradford@ceramem.com

Received 20 January 2000; accepted 4 April 2000

The isothermal, non-oxidative, two-step conversion of CH_4 to C_{2+} hydrocarbons was investigated over unsupported and supported Pt and Ru catalysts at moderate temperatures and elevated pressures. The single-cycle specific activity (μmol C_{2+}/g_{cat}) and total product yield (μmol C_{2+}/μmol surface metal) for Ru powder at 430 K were significantly higher than for Pt powder at 503 K. The activity and total product yield for mixed metal oxide (MMO)-supported Ru were significantly less than for Ru powder; however, Pt/MMO exhibited similar activity and product yield in comparison to Pt powder. The formation of methylbutane and methylpentane increased with increasing pressure over Ru/MMO. However, increasing pressure favored the formation of C_4 species over Pt/MMO.

Keywords: ruthenium, platinum, methane, non-oxidative, two-step conversion

1. Introduction

In 1991, two independent research groups demonstrated the two-step, non-oxidative conversion of CH_4 to C_{2+} alkanes over reduced Group VIII transition metals at temperatures lower than 773 K [1,2]. Since that time, numerous investigations of this two-step route to CH_4 homologation have been reported by researchers at the Université de Nancy [3–10], Eindhoven University of Technology [11–13] and elsewhere [14–28]. During the first step the catalyst is exposed to CH_4, in which both dissociative adsorption to CH_x species and some C–C bond formation occur [29,30]. Hydrogen is subsequently introduced in the second step to hydrogenate the surface carbonaceous deposits and induce alkane desorption, though hydrogenolysis reactions can also occur [30]. A one-step variation of this process, in which CH_4 is pulsed into a dilute H_2 stream, has also been reported [22].

The C_{2+} product distribution and yield during two-step CH_4 homologation are a function of the metal [31], support/metal–support interaction [18], temperature, pressure, space velocity and contact time [7]. For example, it has been shown for SiO_2-supported metals that the C_{2+} product yield, the chain growth probability, and the selectivity to C_{2+} during the hydrogenation step, can be correlated empirically with the heat of adsorption for carbon on the metal surface [31]. For isothermal operation, the C_{2+} product yields over SiO_2-supported Ru, Pt and Co exhibit a maximum at intermediate temperatures [7]. In addition, Paréja et al. have demonstrated that an increase in operating pressure results in a marked shift to higher molecular weight products [32].

Despite this substantial research effort in the area of non-oxidative, two-step CH_4 homologation, a commercial process has not yet been developed. A significant economic hurdle has been that the C_{2+} product distribution typically contains only branched and linear C_2–C_6 alkanes, rather than, for example, significant quantities of olefins or aromatics. Recently, however, the predominant formation of cyclohexane, methylcyclohexane and dimethylcyclohexane over SiO_2-supported Ni–Cu has been reported [32]. In addition, the formation of relatively large quantities of ethylene has been observed over NaY-supported [18] and sol/gel prepared, Al_2O_3-supported [21] Ru catalysts.

Therefore, the main purpose of the preliminary research described herein was to probe the roles of pressure and metal–support interactions on the C_{2+} product distribution. Consequently, the isothermal, non-oxidative, two-step conversion of CH_4 was investigated over unsupported and supported Pt and Ru catalysts at moderate temperatures and elevated pressures.

2. Experimental

2.1. Catalyst preparation and characterization

Nanoparticle Pt (Nanophase Technologies, 99.5+%) and Ru (Aldrich, 99.9+%) powder samples of relatively low dispersion were purchased for use in this investigation. The Pt powder sample contained up to 10 ppm Cu as an impurity; however, detailed analysis on this sample was not performed. The Ru powder sample used herein contained trace levels of Al (5 ppm), Mg (1 ppm) and Cu (1 ppm). These Pt and Ru powders were pretreated *ex situ* following a procedure used previously for Pt powder [33]. Samples were oxidized under flowing 5% O_2 in He for 1 h at 673 K, and subsequently reduced under flowing H_2 (99.999%) for 1 h at 723 K. Thereafter, the samples were cooled to room

temperature under flowing He (99.999%) and subsequently stored in a desiccator for later use. During this pretreatment procedure, gas hourly space velocities of 2400 $cm^3/h\,g_{cat}$ and 1200 $cm^3/h\,g_{cat}$ were used for Pt and Ru, respectively. A portion of the Pt powder was not subjected to this high-temperature pretreatment procedure, but was used as received.

Mixed metal oxide (MMO)-supported Pt and Ru catalysts were prepared via incipient wetness. Prior to use the MMO powder was calcined in a tube furnace under flowing O_2 (99.96%) for 2 h at 773 K. The Ru/MMO and Pt/MMO catalysts were prepared via impregnation of the calcined MMO powder with solutions of $RuCl_3{\cdot}xH_2O$ and $H_2PtCl_6{\cdot}xH_2O$, respectively, dissolved in distilled H_2O. The impregnated samples were then dried overnight in static air at 393 K, calcined under flowing O_2 for 2 h at 773 K, and ultimately stored in a desiccator for later use. Due to the uncertainty of salt hydration number (x) and the possibility of Co contamination (from the ceramic boats used during MMO calcination), metal contents were measured using direct current plasma emission spectroscopy (Luvak Inc.).

The total surface areas of the MMO-supported catalysts, measured using N_2 BET, and the metal dispersions for all catalysts, measured using both H_2 and CO pulse chemisorption, were obtained by Dr. Flytzani-Stephanopoulos and her research group at Tufts University. Prior to either N_2 BET or chemisorption, the samples were pretreated in flowing H_2 (6000 $cm^3/h\,g_{cat}$) for 2 h at 523 K. In addition, temperature-programmed reduction (TPR) of the MMO-supported catalysts ($\beta = 10$ K/min, $N_2/H_2 = 19$, GHSV = 24 000 $cm^3/h\,g_{cat}$) was performed by Dr. Anil Prabhu at Quantachrome Corporation.

2.2. Bench-scale reactor

High-purity CH_4 (99.99%), H_2 (99.999%) and He (99.999%) were introduced independently to the feed-gas manifold. Industrial excess flow valves were installed immediately downstream of the CH_4 and H_2 cylinder regulators to prevent huge leaks of these gases in case of catastrophic instrument failure. All gas exiting the gas manifold passed through a 0.5 μm filter prior to entering a high-pressure metering valve, where it was subsequently directed to either the reactor bypass line or inlet. The reactor was a 1″ diameter 304SS tube. Electrical heating tape (Thermolyne, Insulated Fibrox, $T_{max} = 753$ K) powered by a Glas-Col® PL312 Minitrol was used to control reactor temperature. A portable digital thermometer (Omega, model HH11) was used to monitor reaction temperature from a K-type thermocouple located inside of the catalyst bed. The reactor head assembly included a thermocouple port, a pressure gauge and a safety relief valve (Nupro model SS-4R3A) set at ~750 psig, and was contained within a fume hood. Reactor effluent entered a back-pressure regulator (GO model BP60-1A11CEL1H1), and was then directed to either a rotameter or to the hydrocarbon product trap, which was a 1.125″ diameter 316SS tube suspended in a liquid-N_2 bath. The trap was connected to a pressure gauge and a safety relief valve set at ~750 psig. A valve connected to the product trap was used to introduce gas from the hydrocarbon trap to a manual gas-sampling port.

2.3. Catalyst testing

The performances of Ru powder, Pt powder, Ru/MMO and Pt/MMO for isothermal, two-step CH_4 homologation were examined. Approximately 0.5 g of catalyst was packed into the reactor between plugs of Heraeus® Amersil quartz wool (Friedrich and Dimmock, Inc.). Thereafter the catalyst was purged with He (80 psig, 12 000 $cm^3/h\,g_{cat}$) overnight. The following morning the gas flow was switched to H_2 (100, 400 or 700 psig, 12 000 $cm^3/h\,g_{cat}$), the reactor was heated to 523 K, and the catalyst was reduced for 2 h. Thereafter the catalyst was purged for ~60 min with He (80 psig, 12 000 $cm^3/h\,g_{cat}$) to remove residual H_2 from the system. Near-optimal reaction temperatures of 433 and 523 K were chosen for Ru and Pt, respectively, based on the work of Amariglio et al. [7]. Once at reaction temperature, the catalyst was exposed to flowing CH_4 (100, 400 or 700 psig, ~48 000 $cm^3/h\,g_{cat}$) for either 2 min (Pt powder and Pt/MMO) or 15 min (Ru and Ru/MMO). To remove gas-phase CH_4 from the system prior to hydrogenation, the reactor was then flushed with flowing He (~84 000 $cm^3/h\,g_{cat}$) for 5 min. The reactor effluent was then routed to the liquid-nitrogen trap, and the catalyst was exposed to flowing H_2 (~60 000 $cm^3/h\,g_{cat}$) for 45–60 min.

Upon completion of the second step, i.e., introduction of hydrogen, the liquid-nitrogen trap was isolated, excess H_2 pressure was vented, and the trap was gradually warmed overnight to room temperature. After recording the trap pressure and temperature, the molar amount of gas in the trap was estimated using the calibrated trap volume (24.8 ± 1.2 cm^3) and the ideal gas law. The gas was then sampled with a 1000 μl syringe and manually injected into a gas chromatograph (SRI model 8610) equipped with an 80/120 Carbopack B/3% SP-1500 column and a flame ionization detector. Through a combination of retention time data provided by Supelco [36], in-house calibration data, and published FID sensitivity factor data [37], product quantification was accomplished.

3. Results and discussion

3.1. Catalyst characterization

Metal contents of the MMO-supported catalysts are provided in table 1. Although the atomic ratio of Co/Ru = 0.05 in the Ru/MMO catalyst is fairly small, the ratio of Co/Pt = 0.33 in the Pt/MMO catalyst is significant. Nevertheless, the extent of interaction in these catalysts between

Co, Ru and Pt, if any, is unknown at this time. A summary of the N_2 BET surface areas, chemisorption uptakes, and metal crystallite sizes estimated for each catalyst is provided in table 2. The average particle size of the as-received Pt powder reported by the manufacturer is 23 nm; however, reduction of this Pt powder for 2 h at 523 K increased particle size to 70 ± 24 nm (table 2). *Ex situ* pretreatment in 5% O_2 at 673 K prior to *in situ* reduction further increased the Pt particle size to 163 ± 50 nm. The Ru powder sample, which was also subjected to this *ex situ* pretreatment, exhibited a particle size of 420 ± 140 nm. The surface-weighted particle sizes of the MMO-supported Pt and Ru particles were calculated assuming negligible H_2 and CO chemisorption onto Co. Considering that the Co was introduced accidentally during calcination of the MMO support in the solid state, an assumption of poor Co dispersion and low adsorption capacity seems reasonable. Nevertheless, with this uncertainty, the calculated particle sizes for Ru and Pt in the MMO-supported samples must be considered as lower-limit estimates. Regardless, it is interesting to note that the irreversible H_2 uptakes were considerably higher than the corresponding CO uptakes on the MMO-supported samples. Although it is possible that residual Cl from the metal salt precursors is present on the MMO-supported catalysts after reduction at 523 K, the presence of Cl on Ru, for example, more strongly suppresses H_2 rather than CO adsorption [38]. Thus, the relatively higher hydrogen adsorption capacity is not likely due to the presence of Cl. Possibly, this phenomenon is due to hydrogen spillover onto the support surface during chemisorption. The formation of stable $(Ti–H)^{3+}$ species on, e.g., reduced TiO_2 surfaces, has been reported [39].

Temperature-programmed reduction (TPR) spectra for Ru/MMO and Pt/MMO are shown in figure 1. A temperature maximum was observed in the TPR spectrum for Ru/MMO at ca. 505 K, indicating that *in situ* reduction in H_2 at 523 K (used for the CH_4 homologation experiments) is sufficient to reduce this catalyst. In contrast to this, two temperature maxima were observed, at ca. 425 and 800 K, for the Pt/MMO catalyst. It is tentatively presumed that the peak near 425 K is due to the reduction of Pt, and that the remainder of the TPR spectrum is indicative of the partial reduction of the support and/or Co. If the latter postulate is correct, then this TPR spectrum is evidence for hydrogen spillover, and possibly either metal–support or Pt–Co interactions, in the Pt/MMO catalyst. Similar reduction behavior has been observed for numerous other supported catalysts, such as Pt/TiO_2 [35].

Table 1
Bulk metal composition of MMO-supported catalysts.

Catalyst	Metal content (wt%)		
	Pt	Co	Ru
Pt/MMO	1.01 ± 0.02	0.10 ± 0.01	–
Ru/MMO	–	0.056 ± 0.005	1.85 ± 0.05

3.2. Catalyst performance

The single-cycle performances of the Ru and Pt catalysts for isothermal, two-step CH_4 homologation are shown in table 3. Both Ru/MMO and Pt/MMO exhibited an apparent maximum in activity for CH_4 homologation at a pressure of ca. 400 psig; consequently, the Pt and Ru powder samples were examined only at this pressure. It is of interest that, over Ru/MMO, an increase in pressure from 100 to 700 psig resulted in a concomitant increase in both n-C_5H_{12} and branched alkane ($<n$-C_5 and $>n$-C_5) production. Similar results with respect to pressure have been observed previously over $Ni–Cu/SiO_2$ [32]. The unsupported Ru powder sample exhibited an activity for CH_4 homologation significantly higher than Ru/MMO (table 3). In addition, the Ru powder exhibited a higher molecular weight product distribution than Ru/MMO; i.e., the dominant C_{2+} alkane over Ru/MMO was ethane, while over Ru powder it was n-pentane. A more interesting result was that over Ru/MMO at 100 psig, there was a significant increase in C_4 production (table 3). The major C_4 species eluted in the gas chromatograph at a retention time between those of isobutane and n-butane, corresponding to C_4 olefins [36]; however, definitive assignment of these species is not possible at this time and is dependent upon future GC/MS studies. The Pt/MMO catalyst exhibited higher activity than Ru/MMO and Pt powder on a per gram catalyst basis (table 3). More

Table 2
BET surface areas (S), chemisorption uptakes, metal dispersions and particle sizes for Ru and Pt catalysts.

Catalyst	S	Uptake (μmol/g_{cat})		Dispersion (%)[a]		Particle size (nm)[b]	
	(m^2/g)	H_2	CO	H_2	CO	H_2	CO
MMO	4.9	–	–	–	–	–	–
Pt/MMO	5.2	59 ± 24	35.4 ± 2.2	100	68 ± 4	1.1	1.7 ± 0.1
Ru/MMO	5.3	38 ± 26	6.0 ± 0.3	42 ± 28	3.3 ± 0.2	2.7	34 ± 2
Pt powder	–	–	24.3	–	0.75 ± 0.25	–	163 ± 50
Pt powder[c]	–	45	59 ± 8	1.8	1.8 ± 0.6	63	70 ± 24
Ru powder	–	–	15.3	–	0.3 ± 0.1	–	420 ± 140

[a] Metal dispersions for Pt/MMO and Ru/MMO are calculated assuming the adsorption stoichiometry of $H_{ad}/metal_{surf} = CO_{ad}/metal_{surf} = 1$. Mean values reported for Pt and Ru powder result from assumed stoichiometries of 1 and $1/2$; the stoichiometry of $1/2$ has been observed for CO adsorption on Pt(111) and low surface area Pt powder [33,34].

[b] Surface-weighted particle size (d_s) calculated from dispersion (D) using d_s (nm) $= 113/D$ (%). From [35].

[c] This sample was not subject to *ex situ* oxidization at 673 K and reduction at 723 K prior to analysis.

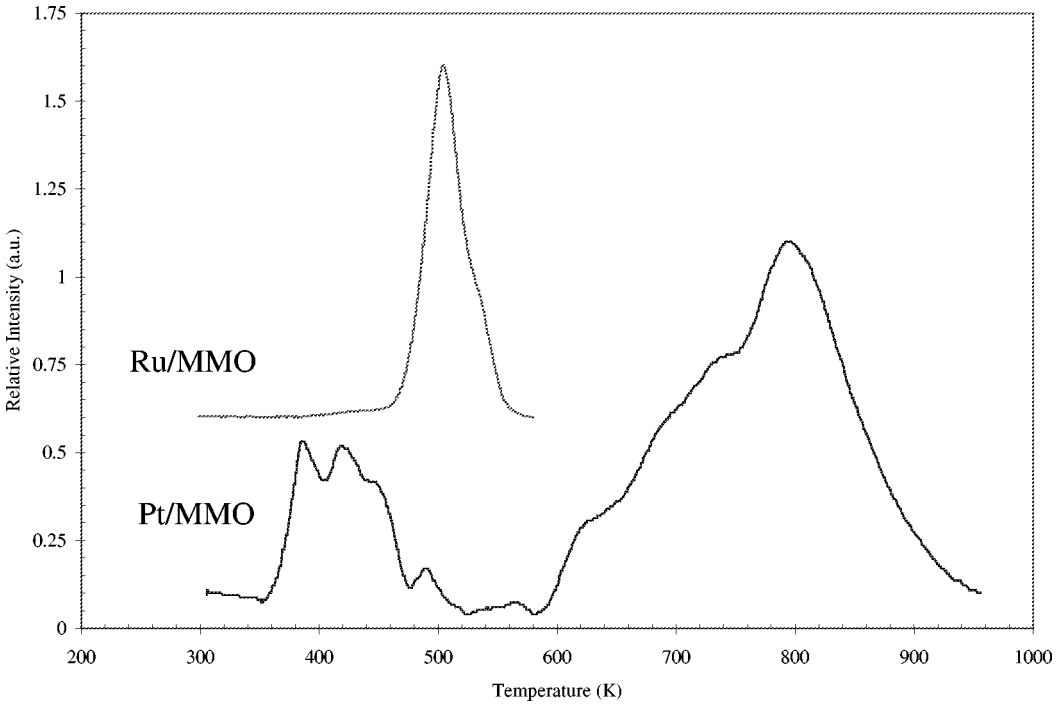

Figure 1. Temperature-programmed reduction (TPR) spectra for Ru/MMO and Pt/MMO. Conditions: GHSV = 24 000 $cm^3/h\,g_{cat}$, $N_2/H_2 = 19$, $P = 1$ atm, $\beta = 10$ K/min.

interesting, however, is that at 700 psig over Pt/MMO the major products in the C_{2+} distribution were C_4 species.

A comparison of C_{2+} product distributions reported herein over Ru/MMO with data reported over Ru/SiO_2 is shown in figure 2. Excluding data for Ru/MMO at 100 psig, for which there was a significant promotion of C_4 formation, the data in figure 2 illustrate a shift in the product distribution to higher molecular weights with increasing pressure, as mentioned previously. The C_{2+} product distributions obtained during isothermal, two-step CH_4 homologation over Pt powder at 492 K and 400 psig, and Pt/SiO_2 at 473–523 K and 0 psig [40] are compared in figure 3. Typically, there are negligible metal–support interactions for SiO_2-supported Pt after reduction at 523 K; consequently, SiO_2-supported Pt particles should exhibit similar catalytic behavior (regarding CH_4 activation) to unsupported Pt powder [41]. Nevertheless, a notable difference is that the Pt powder exhibited a slightly lower C_{4-} yield and a slightly higher C_{5+} yield. Presumably this is a direct consequence of the negative H_2 pressure dependence on hydrogenolysis over Pt; i.e., the rates of hydrogenolysis of C_2–C_5 alkanes over Pt typically decrease with increasing H_2 partial pressure [42].

It is also of interest to compare the catalyst turnover numbers (TON); i.e., the moles of surface C converted to C_{2+} per mole of surface metal atom, per cycle. A true turnover frequency cannot be calculated for two-step CH_4 homologation, because the process is not truly catalytic [4]. Koerts et al. studied two-step CH_4 homologation at atmospheric pressure by adsorbing CH_4 at 723 K and hydrogenating the carbon deposits at 373 K [13]; it is possible to calculate a TON of 0.027 for Ru/SiO_2 using their data. This agrees well with the TON range of 0.018–0.051 measured for Ru/MMO in this investigation (table 3). The TON of 0.190 for Ru powder in this study is higher than for either Ru/MMO or Ru/SiO_2. Possibly, this is indicative of either a metal particle size effect, an inhibiting effect of MMO on the activity of dispersed Ru, an inhibiting effect of adsorbed Cl on the Ru/MMO catalyst or the influence of pressure (in regard to Ru/SiO_2). However, none of these possibilities can be excluded at this time. A TON of 0.001 for Pt/SiO_2 can also be calculated from the data of Koerts et al. [13]. However, this value is over an order of magnitude less than the TON range of 0.010–0.026 measured for Pt powder and Pt/MMO in this investigation (table 3). Possibly the difference is due to reaction conditions, most notably, the higher pressures and lower CH_4 adsorption temperatures used herein.

With this limited information it is possible to speculate about some mechanistic aspects of two-step CH_4 conversion over MMO-supported Pt. In general, CH_4 dissociation over a supported Group VIII metal should yield a distribution of CH_x (or C_mH_n) species. For example, it is possible that CH_4 dissociation over Pt/MMO at elevated pressures ($400 \leqslant P$ (psig) $\leqslant 700$) results in the formation of some CH_2 species on the Pt surface:

$$CH_4 + 4M \rightarrow CH_2\text{–}M_2 + 2H\text{–}M \qquad (1)$$

where M is a surface Pt atom. Each CH_2 surface fragment in equation (1) is considered bonded to two surface metal atoms (M_2) because CH_x fragments on Pt tend to complete their tetravalency if an appropriate site is available [43]. For two-step CH_4 homologation, surface CH_x species with

Table 3
Total CH_4 homologated and C_{2+} product distribution for isothermal, two-step CH_4 homologation over unsupported and MMO-supported Ru and Pt.

Catalyst	Reaction conditions[a]					Experimental results									
	T (K)		GHSV ($cm^3/h\,g_{cat}$)		P	Homologated CH_4		C_{2+} product distribution (wt%)							
	CH_4[b]	H_2[c]	CH_4	H_2	(psig)	μmol/g_{cat}	C/M_{surf}[d]	C_2H_6	C_3H_8	C_4			n-C_5H_{12}	other[e]	
										i-C_4H_{10}	$C_4^=$	n-C_4H_{10}		$<n$-C_5	$>n$-C_5
Ru/MMO	431 ± 3	433 ± 3	98 000[f]	14 900[g]	100	0.10 ± 0.06	0.017	41.0 ± 1.8	13.6 ± 4.1	6.5 ± 1.5	17.2 ± 2.6	12.4 ± 0.6	8.3 ± 0.1	0.9 ± 0.9	0 ± 0
	432 ± 4	434 ± 7	47 300	59 100	400	0.29 ± 0.03	0.048	46.2 ± 1.5	12.6 ± 2.2	1.9 ± 0.3	0.4 ± 0.4	13.6 ± 2.0	19.2 ± 2.2	5.7 ± 0.3	0.4 ± 0.4
	427 ± 9	433 ± 7	47 400	59 200	700	0.17 ± 0.01	0.028	27.5 ± 0.5	15.1 ± 1.2	2.1 ± 0.2	1.1 ± 1.0	15.1 ± 1.5	22.9 ± 0.4	8.8 ± 0.1	7.3 ± 2.0
Ru	427 ± 8	430 ± 6	48 000	60 000	400	2.9 ± 1.7	0.190	22.6 ± 1.0	7.8 ± 0.1	1.3 ± 0.1	0.5 ± 0.2	13.3 ± 0.2	34.9 ± 0.0	8.1 ± 0.1	11.7 ± 0.9
Pt/MMO	506 ± 12	522 ± 15	47 100	58 900	400	0.98 ± 0.01	0.028	43.3 ± 1.8	5.4 ± 0.4	0.8 ± 0.1	32.6 ± 4.0	2.2 ± 0.2	3.2 ± 1.4	4.8 ± 1.2	6.5 ± 0.2
	483 ± 29	516 ± 28	46 300	58 000	700	0.50 ± 0.06	0.014	26.7 ± 2.5	2.7 ± 0.3	1.0 ± 0.1	62.9 ± 3.1	0.8 ± 0.1	0.6 ± 0.1	1.3 ± 0.1	4.0 ± 0.1
Pt[h]	492 ± 25	514 ± 14	47 600	59 500	400	0.57 ± 0.01	0.010	60.8 ± 2.8	1.7 ± 0.1	0.3 ± 0.1	3.6 ± 0.5	0.6 ± 0.2	15.2 ± 1.4	8.3 ± 1.5	9.5 ± 2.7

[a] All catalyst samples were pretreated *in situ* for 2 h at 523 K prior to reaction.
[b] Temperature during dissociative CH_4 adsorption ($\pm 1\sigma_n$).
[c] Temperature during hydrogenation.
[d] Atomic ratio of carbon homologated to C_{2+} to exposed surface metal atoms (as measured by CO chemisorpiton – see table 2).
[e] The "other" sub-group refers to species which elute in the GC analysis prior to ($<n$-C_5) and after ($>n$-C_5) n-C_5H_{12}. The $<n$-C_5 species are most likely methylbutane and either cyclopentane or pentene. The $>n$-C_5 species are mostly methylpentane.
[f] This GHSV is from an average of two different experiments at 5960 and 190 200 $cm^3/h\,g_{cat}$.
[g] This GHSV is from an average of two different experiments at 5960 and 27 800 $cm^3/h\,g_{cat}$.
[h] This sample was not subject to *ex situ* oxidization at 673 K and reduction at 723 K.

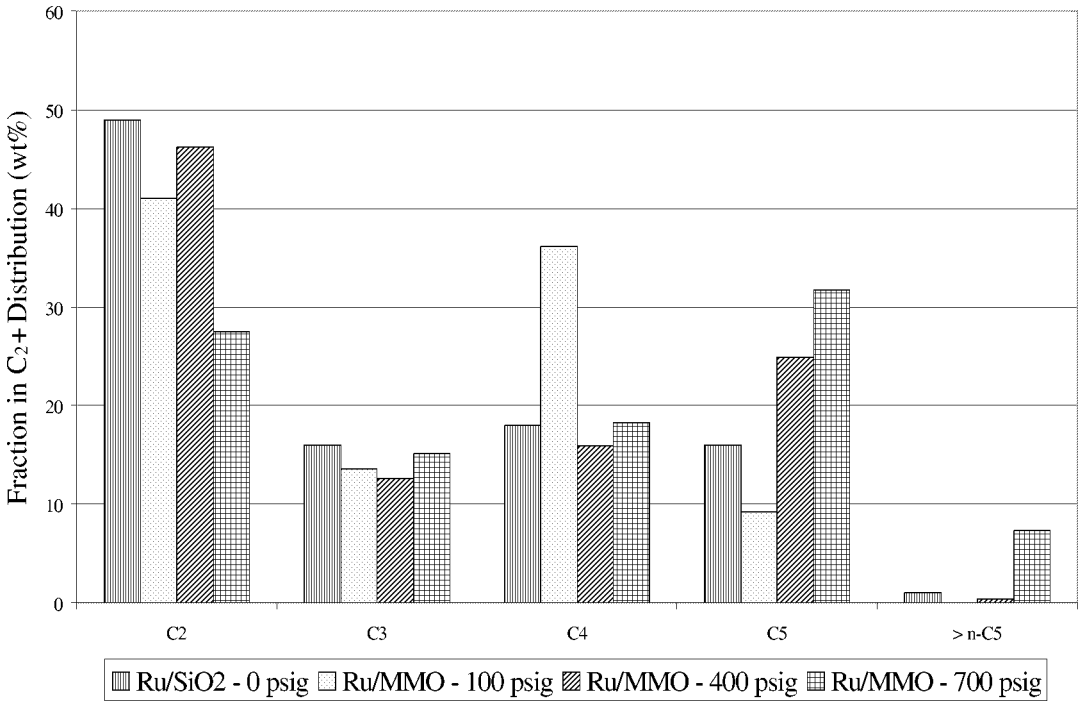

Figure 2. A comparison of C_{2+} product distributions during isothermal, two-step CH_4 homologation at 423–433 K over Ru/MMO (table 3) and Ru/SiO_2 [40]. Note that n-C_5H_{12} and $<n$-C_5 species listed in table 3 have been lumped together as C_5 species in this figure.

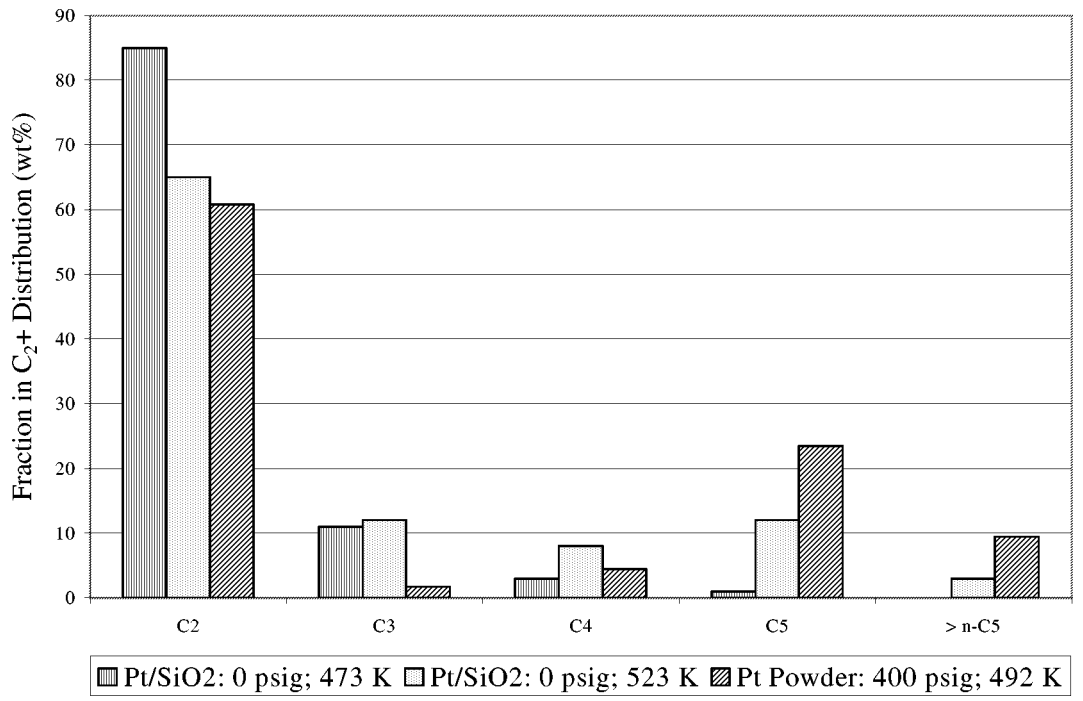

Figure 3. A comparison of C_{2+} product distributions during isothermal, two-step CH_4 homologation over Pt powder (table 3) and Pt/SiO_2 [40]. Note that n-C_5H_{12} and $<n$-C_5 species listed in table 3 have been lumped together as C_5 species in this figure.

$1 < x \leqslant 2$ (or C_mH_n species with $1 < n/m \leqslant 2$) are believed to be optimal for the production of higher hydrocarbons [22]. In addition, it is of interest to note that kinetic data for CO_2 reforming of CH_4 over supported Pt catalysts at temperatures less than 723 K are explained well by a model derived from a mechanism which includes surface CH_2 species as the main CH_x reaction intermediate [44].

Carbon–carbon bond formation may occur during CH_4 adsorption, as mentioned previously. The BOC/MP-estimated [45] heats of adsorption for ethane (5 kcal/mol), ethylene (12 kcal/mol), and acetylene (14 kcal/mol) on Pt

are significantly less than, for example, CH_2 (68 kcal/mol), H_3C–C (97 kcal/mol) and H_3C–CH (70 kcal/mol). Consequently, on the basis of simple desorption theory, the surface coverages of ethane, ethylene and acetylene on Pt at 523 K should be significantly less than those of CH_2, H_3C–C and H_3C–CH [46]. Assuming the presence of these species on the catalyst surface after dissociative CH_4 adsorption, introduction of hydrogen during the second step of the two-step homologation sequence could induce several reactions to occur, such as the recombinative desorption of CH_2 as ethylene,

$$2CH_2\text{–}M_2 \rightarrow C_2H_4 + 2M \quad (2)$$

which could be subsequently either hydrogenated on the Pt surface to produce ethane,

$$C_2H_4 + H_2 \rightarrow C_2H_6 \quad (3)$$

or dimerized to butenes,

$$2C_2H_4 \rightarrow C_4H_8 \quad (4)$$

Alternatively, it is possible that surface C_mH_n species, such as H_3C–C and H_3C–CH, are formed during CH_4 dissociation:

$$2CH_4 + 8M \rightarrow H_3C\text{–}C\text{–}M_3 + 5H\text{–}M \quad (5)$$

$$2CH_4 + 6M \rightarrow H_3C\text{–}CH\text{–}M_2 + 4H\text{–}M \quad (6)$$

Both H_3C–C and H_3C–CH have H/C ratios within the proposed optimal range of 1–2, and, presumably, may undergo numerous reactions, such as hydrogenation and hydrogen-assisted recombinative desorption, to yield C_2 and C_4 products.

Thermodynamically, both ethylene hydrogenation and dimerization are favored with increasing pressure. In addition, the ethylene reaction order for hydrogenation over supported Pt is apparently negative or zero at pressures higher than 75 Torr [47]. Therefore, the observed increase in C_4 selectivity over Pt/MMO with increasing reaction pressure may be due simply to intrinsic kinetics.

There are insufficient experimental and theoretical data available at this time to explain why C_{2+} olefins, in particular C_4 olefins, may form and survive in the H_2-rich environment which exists during the second step of the two-step homologation process. Nevertheless, it is worth noting that in previous investigations of two-step CH_4 homologation, significant ethylene formation has been observed over supported Ru [18,21], and butene formation has been observed over Pd–Co/SiO_2 [22]. Possibly, Pt–Co and metal–support interactions exist in the reduced Pt/MMO catalyst which create sites necessary to promote C_4 olefin formation. Clearly, however, more work needs to be done before any non-speculative conclusion can be reached.

4. Summary

The isothermal, non-oxidative, two-step conversion of CH_4 to C_{2+} hydrocarbons was investigated over unsupported and supported Pt and Ru catalysts at moderate temperatures and elevated pressures. The experimental results reported herein indicate that unsupported and SiO_2-supported Pt exhibit a similar product distribution for isothermal, two-step CH_4 homologation. Product yields for Pt/MMO, however, were slightly higher than those for either Pt/SiO_2 or Pt powder. Conversely, product yields for Ru powder were larger than those observed for either Ru/MMO or Ru/SiO_2. More importantly, the data herein demonstrate that use of a support which exhibits mild metal–support interactions can shift the product distribution. In addition, in agreement with earlier studies, it was shown that an increase in reaction pressure increases the branching and molecular weight distribution of the product.

Acknowledgement

This work was funded by the National Science Foundation under SBIR Grant No. DMI-9861211. The author would like to thank Dr. Maria Flytzani-Stephanopoulos and her research group at Tufts University for BET and chemisorption measurements, Dr. Anil Prabhu at Quantachrome Corporation for TPR measurements, and CeraMem Corporation for permission to publish this work.

References

[1] M. Belgued, P. Paréja, A. Amariglio and H. Amariglio, Nature 352 (1991) 789.
[2] T. Koerts and R.A. van Santen, J. Chem. Soc. Chem. Commun. (1991) 1281.
[3] M. Belgued, S. Monteverdi, P. Paréja, H. Amariglio, A. Amariglio and J. Saint-Just, in: *Preprints, Symposium on Natural Gas Upgrading II*, Vol. 37 (Division of Petroleum Chemistry, Inc., Am. Chem. Soc., 1992) p. 324.
[4] E. Mielczarski, S. Monteverdi, A. Amariglio and H. Amariglio, Appl. Catal. A 104 (1993) 215.
[5] A. Amariglio, P. Paréja, M. Belgued and H. Amariglio, J. Chem. Soc. Chem. Commun. (1994) 561.
[6] H. Amariglio and J. Saint-Just, US Patent 5,414,176 (1995).
[7] H. Amariglio, J. Saint-Just and A. Amariglio, Fuel Process. Technol. 42 (1995) 291.
[8] M. Belgued, A. Amariglio, P. Paréja and H. Amariglio, J. Catal. 159 (1996) 441, 449.
[9] M. Belgued, A. Amariglio, L. Lefort, P. Paréja and H. Amariglio, J. Catal. 161 (1996) 282.
[10] P. Paréja, S. Molina, A. Amariglio and H. Amariglio, Appl. Catal. A 168 (1998) 289.
[11] T. Koerts and R.A. van Santen, J. Mol. Catal. 70 (1991) 119.
[12] T. Koerts and R.A. van Santen, in: *Preprints, Symposium on Natural Gas Upgrading II*, Vol. 37 (Division of Petroleum Chemistry, Inc., Am. Chem. Soc., 1992) p. 336.
[13] T. Koerts, M.J.A.G. Deelen and R.A. van Santen, J. Catal. 138 (1992) 101.
[14] M.-C. Wu, P. Lenz-Solomun and J.G. Goodwin, Jr., J. Vac. Sci. Technol. A 12 (1994) 2205.
[15] N. Cheikhi, M. Ziyad, G. Coudurier and J.C. Védrine, Appl. Catal. A 118 (1994) 187.
[16] L. Guczi, R.A. van Santen and K.V. Sarma, Catal. Rev. Sci. Eng. 38 (1996) 249.

[17] L. Guczi, K.V. Sarma and L. Borkó, Catal. Lett. 39 (1996) 43.
[18] L. Guczi, Zs. Koppány, K.V. Sarma, L. Borkó and I. Kiricsi, Stud. Surf. Sci. Catal. 105 (1997) 861.
[19] L. Guczi, K.V. Sarma, Zs. Koppány, R. Sundararajan and Z. Zsoldos, Stud. Surf. Sci. Catal. 107 (1997) 333.
[20] L. Guczi, K.V. Sarma and L. Borkó, J. Catal. 167 (1997) 495.
[21] L. Guczi, G. Stefler, Zs. Koppány, L. Borkó, S. Niwa and F. Mizukami, Appl. Catal. A 106 (1997) L29.
[22] L. Guczi, L. Borkó, Zs. Koppány and F. Mizukami, Catal. Lett. 54 (1998) 33.
[23] G.-C. Shen and M. Ichikawa, J. Chem. Soc. Faraday Trans. 93 (1997) 1185.
[24] O. Garnier, J. Shu and P.A. Grandjean, Ind. Eng. Chem. Res. 36 (1997) 554.
[25] G. Boskovic, J.S.M. Zadeh and K.J. Smith, Catal. Lett. 39 (1996) 163.
[26] G. Boskovic, J.S.M. Zadeh and K.J. Smith, Stud. Surf. Sci. Catal. 107 (1997) 263.
[27] J.S.M. Zadeh and K.J. Smith, J. Catal. 176 (1998) 115.
[28] F. Solymosi and J. Cserényi, Catal. Lett. 34 (1995) 343.
[29] Z. Hlavathy, Z. Paál and P. Tétényi, J. Catal. 166 (1997) 118.
[30] A. Amariglio, P. Paréja and H. Amariglio, J. Catal. 166 (1997) 121.
[31] M.C.J. Bradford, J. Catal. 189 (2000) 238.
[32] F. Simon, S. Molina, A. Amariglio, P. Paréja, H. Amariglio and G. Szabo, Catal. Today 46 (1998) 217.
[33] M.C.J. Bradford and M.A. Vannice, Catal. Lett. 48 (1997) 31.
[34] G. Ertl, M. Neumann and K.M. Streit, Surf. Sci. 64 (1977) 393.
[35] M.C.J. Bradford and M.A. Vannice, J. Catal. 173 (1998) 157.
[36] Supelco, Inc., Bulletin 816B, 1996.
[37] W.A. Dietz, J. Gas Chromatogr. (1967) 68.
[38] M.C.J. Bradford and M.A. Vannice, J. Catal. 183 (1999) 69.
[39] J. Sanz, M. Rojo, P. Malet, G. Munuera, M.T. Blasco, J.C. Conesca and J. Soria, J. Phys. Chem. 89 (1985) 5427.
[40] H. Amariglio, P. Paréja and A. Amariglio, Catal. Today 25 (1995) 113.
[41] M.C.J. Bradford and M.A. Vannice, Catal. Today 50 (1999) 87.
[42] G.A. Somorjai, *Introduction to Surface Chemistry and Catalysis* (Wiley, New York, 1994).
[43] C. Minot, M.A. van Hove and G.A. Somorjai, Surf. Sci. 127 (1982) 441.
[44] M.C.J. Bradford and M.A. Vannice, Catal. Rev. Sci. Eng. 41 (1999) 1.
[45] E. Shustorovich, Adv. Catal. 37 (1990) 101.
[46] P.A. Redhead, Vacuum 12 (1962) 203.
[47] R.D. Cortright, S.A. Goddard, J.E. Rekoske and J.A. Dumesic, J. Catal. 127 (1991) 342.